

Machine Learning-Based Classification of Subjective Cognitive Decline, Mild Cognitive Impairment, and Alzheimer's Dementia Using Neuroimage and Plasma Biomarkers

Shu-I Chiu, Ling-Yun Fan, Chin-Hsien Lin, Ta-Fu Chen, Wee Shin Lim, Jyh-Shing Roger Jang, and Ming-Jang Chiu*



Cite This: *ACS Chem. Neurosci.* 2022, 13, 3263–3270



Read Online

ACCESS |

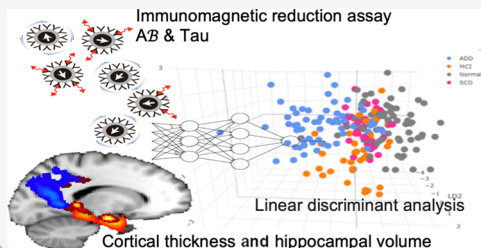
Metrics & More

Article Recommendations

Supporting Information

ABSTRACT: Alzheimer's disease (AD) progresses relentlessly from the preclinical to the dementia stage. The process begins decades before the diagnosis of dementia. Therefore, it is crucial to detect early manifestations to prevent cognitive decline. Recent advances in artificial intelligence help tackle the complex high-dimensional data encountered in clinical decision-making. In total, we recruited 206 subjects, including 69 cognitively unimpaired, 40 subjective cognitive decline (SCD), 34 mild cognitive impairment (MCI), and 63 AD dementia (ADD). We included 3 demographic, 1 clinical, 18 brain-image, and 3 plasma biomarker ($\text{A}\beta_{1-42}$, $\text{A}\beta_{1-40}$, and tau protein) features. We employed the linear discriminant analysis method for feature extraction to make data more distinguishable after dimension reduction. The sequential forward selection method was used for feature selection to identify the 12 best features for machine learning classifiers. We used both random forest and support vector machine as classifiers. The area under the receiver operating curve (AUROC) was close to 0.9 between diseased (combining ADD and MCI) and the controls. AUROC was higher than 0.85 between SCD and controls, 0.90 between MCI and SCD, and above 0.85 between ADD and MCI. We can differentiate between adjacent phases of the AD spectrum with blood biomarkers and brain MR images with the help of machine learning algorithms.

KEYWORDS: *Alzheimer's disease spectrum, mild cognitive impairment, subjective cognitive decline, machine learning, neuroimage, plasma biomarker*



INTRODUCTION

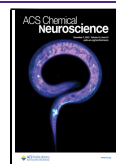
Alzheimer's disease (AD) is the most important cause of dementia in the elderly population, and the pathological hallmarks are intraneuronal tau accumulations as neurofibrillary tangles and extracellular amyloid plaques depositions. AD is now considered a disease that progresses continuously from the preclinical stage to the prodromal phase and finally to dementia. The process begins years, if not decades, before the diagnosis of clinical dementia.¹ While the pathology of the asymptomatic stage of preclinical AD can be evidenced only by neuroimaging or cerebrospinal fluid (CSF) biomarkers, the AD prodromal stage may be defined by single- or multi-domain cognitive impairment without impairment to daily functions. The cognitive impairment is usually episodic memory, so-called single-domain amnestic mild cognitive impairment (MCI), or multi-domain MCI by combining other cognitive dysfunctions. MCI can further be confirmed by neuroimaging or fluid biomarkers. Previous evidence based on a large population demonstrated that the progression from MCI to dementia ranged from 20 to 60%, especially in the amnestic multi-domain subtypes.² The annual conversion rates were 10–15%.³

Subjective cognitive decline (SCD) is characterized by a self-reported cognitive decline with unimpaired cognitive test results.^{4,5} Several studies have suggested that subjects with SCD may be more likely to develop MCI and dementia.^{6–8} Therefore, some subjects with SCD may be in the AD preclinical stage, and the self-experienced cognitive decline compared to previous performance may be a warning sign of clinical dementia. One previous study showed that SCD complaints might be the early manifestation of MCI, a precursor of multiple types of dementia,⁹ including AD. Thus, it is crucial to detect early indications in SCD and MCI to prevent or modify cognitive decline progression. Although there is no cure or effective disease-modifying therapy for AD, we must identify subjects with prodromal even preclinical stages of AD to obtain better therapeutic effects for future

Received: April 27, 2022

Accepted: October 26, 2022

Published: November 15, 2022



disease-modifying treatment. Despite available definitions of each stage of the AD continuum by pathology, cognitive functions, activities of daily living (ADL), instrumental daily activities (IADL), neuroimages, and fluid biomarkers,¹⁰ it is sometimes challenging to determine a boundary between adjacent phases of AD on clinical grounds. In formulating the clinical diagnosis, a clinician would consider the cognitive test results, ADL/IADL assessments, findings of neuroimages, and reports from their family or close friends. Therefore, the diagnosis is not straightforward, even though we have those clinical or research diagnostic criteria. One of the effective tools for clinical validation is the nature course of disease, but it takes a longitudinal observation of months or years. Thus, the application of artificial intelligence technology to assist classification is warranted. Previous studies using machine learning or other computational approaches in diagnosing and monitoring AD included detecting AD from healthy controls,¹¹ measuring disease severity,¹² predicting conversion from MCI to dementia,¹³ and differential diagnosis from other types of dementia.^{11,14,15}

Dimensionality reduction is widespread preprocessing in high-dimensional data analysis, visualization, and modeling.¹⁶ However, high-dimensional data are problematic for classification algorithms due to high computational cost and memory usage.¹⁷ Besides, high dimension data are susceptible to the "curse of dimensionality," which refers to problems that arise when working with high-dimensional data. Prevalent difficulties related to training machine learning models due to high dimensional data are "data sparsity" and "distance concentration", especially in data sets with a relatively small number of samples and large numbers of features.

There are two dimensionality reduction techniques: feature extraction (also known as dimensionality reduction explicitly or feature transformation) and feature selection.¹⁶ Our previous study applied feature extraction to reduce dimension and constructed models by machine learning algorithms to differentiate the disease groups effectively.^{15,18} It also reflected the disease severity in different groups using blood biomarkers.^{15,18} Feature selection is a preprocessing technique that identifies the critical features of a given problem.¹⁹ It can reduce dimensionality and help us understand the causes of disease.¹⁹ We then applied feature selection to identify essential features²⁰ and subject these chosen features to different classifiers. Finally, we used some metrics to evaluate the performance of the two classifiers. Further correlation with the clinical relevance is needed to identify compelling features for the differential diagnosis of subjects with preclinical (SCD), prodromal (MCI), and dementia in the AD continuum.

RESULTS

Participants in the AD dementia (ADD) group were significantly older than those in the control and MCI groups ($p < 0.05$); therefore, we controlled the age effect in the following between-group analysis for plasma and image biomarkers. There was no significant between-group difference for gender distribution. ADD and MCI groups had lower MMSE scores than the control or SCD groups ($p < 0.05$; Table 1). As for the plasma biomarkers, both ADD and MCI groups had higher plasma tau levels than the control group ($p < 0.001$; Figure 1A). For plasma $\text{A}\beta_{1-40}$, all three clinical groups had lower levels than the control group (all $p < 0.05$; Figure 1B), and the $\text{A}\beta_{1-42}/\text{A}\beta_{1-40}$ ratios of the three clinical groups shared the same relative relationship with the control group

Table 1. Demographic, Clinic, and Biomarker Data of Subjects^a

	control	SCD	MCI	ADD
age (years)	65.5 ± 8.6	67.6 ± 6.3	67.5 ± 9.5	71.2 ± 9.7 ^{\$}
gender (F/M)	46/23	20/20	16/18	33/30
education (years)	12.5 ± 4.7	14.5 ± 4.1	11.5 ± 4.7	12.0 ± 3.5
CDR	0	0.5 (M = 0.5)	0.5	0.5/1 (56/7)
MMSE	28.7 ± 1.2	29 ± 0.9	27.1 ± 2.9 [#]	24.9 ± 4.3 [#]
tau (pg/mL)	16 ± 8.7	20.5 ± 4.9	26.1 ± 10.5 ^{**}	32.4 ± 10.9 ^{**}
$\text{A}\beta_{1-40}$ (pg/mL)	60.2 ± 14.3	44.8 ± 9.6*	48.1 ± 17.4*	50.0 ± 17.2*
$\text{A}\beta_{1-42}$ (pg/mL)	15.3 ± 1.8	16.9 ± 5.8	16.2 ± 2.2	17.7 ± 2.8
$\text{A}\beta_{1-42}/\text{A}\beta_{1-40}$	0.27 ± 0.87	0.37 ± 0.11*	0.39 ± 0.13*	0.42 ± 0.31*

^aCDR, clinical dementia rating; MMSE, mini-mental state examination; SCD, subjective cognitive decline; MCI, mild cognitive impairment; ADD, Alzheimer's disease dementia. Compared with control group (*: $p < 0.05$, **: $p < 0.001$); Compared with SCD group (#: $p < 0.05$); Compared with MCI group (: $p < 0.05$).

(all $p < 0.05$; Figure 1D). For $\text{A}\beta_{1-42}$, only ADD reached a significant difference compared to the controls ($p < 0.05$; Table 1 and Figure 1C).

The image biomarkers were the so-called AD-signature areas in terms of hippocampal volume and cortical thickness of these regions of interest. Both ADD and MCI groups had smaller hippocampi as compared to the control ($p < 0.001$) or SCD groups ($p < 0.05$ or 0.01). Regarding the AD signature areas' cortical thickness, most of the significant between-group difference was between ADD, MCI, and the control group ($p < 0.05$ or 0.01). Only two regions showed significant differences between SCD and the control group, the left anterior cingulate, and left precuneus cortices ($p < 0.05$).

Feature Extraction and Feature Selection. **Feature Extraction.** We used the linear discriminant analysis (LDA) method to project data onto a lower-dimensional space with good class separability to visualize the data distribution. LDA reduced the dimensionality to three; the best three combined (transformed) features (i.e., LD1, LD2, and LD3) place the samples in a 3D space that is easier for further classification (Figure 2). The three combined features are new features in the reduced dimensionality. We classified the data set into four classes according to disease severity (i.e., controls, SCD, MCI, and ADD). We used leave-one-out cross-validation (LOOCV) to objectively estimate our model construction procedure's performance. The accuracy with the three linear discriminant variables (LD1 + LD2 + LD3) was higher than those with one (LD1) and two (LD1 + LD2), with an accuracy of 0.76 (Figure S1).

Feature Selection. We performed feature selection using the sequential forward selection (SFS) wrapper method to obtain a subset of relevant features. First, we used the random forest (RF) classifier as an evaluation algorithm to find the most optimal number of features. The evaluation metric was accuracy. We found that 12 features were the best subset number in terms of accuracy (0.69). The best 12 features included total scores of MMSE, age, cortical thickness of the left precuneus, plasma $\text{A}\beta_{1-40}$ level, the volume of the left hippocampus, cortical thickness of the right angular gyrus, left entorhinal gyrus, plasma total tau level, the volume of the right

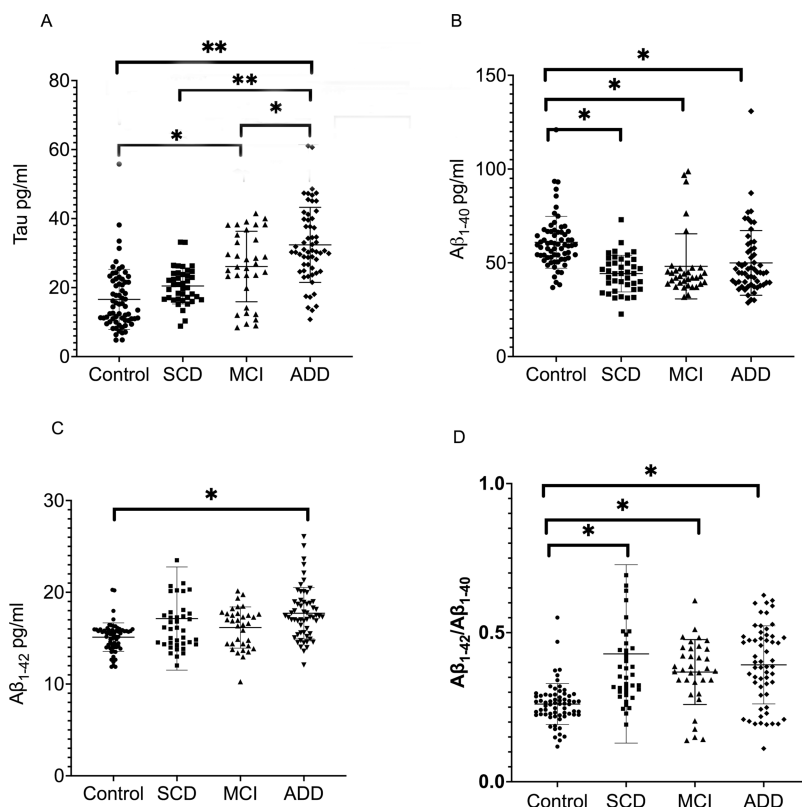


Figure 1. (A) Plasma tau protein levels of all groups with significant differences between ADD, MCI and Control; (B) Plasma $A\beta_{1-40}$ levels of all groups with significant differences between control and all other three groups; (C) Plasma $A\beta_{1-42}$ levels with significant difference only between ADD and Control; (D) $A\beta_{1-42}/A\beta_{1-40}$ ratios of all groups with significant differences between control and all other three groups. SCD: subjective cognitive decline, MCI: mild cognitive impairment, ADD: Alzheimer's disease dementia. Compared with the control group (*: $p < 0.05$, **: $p < 0.001$).

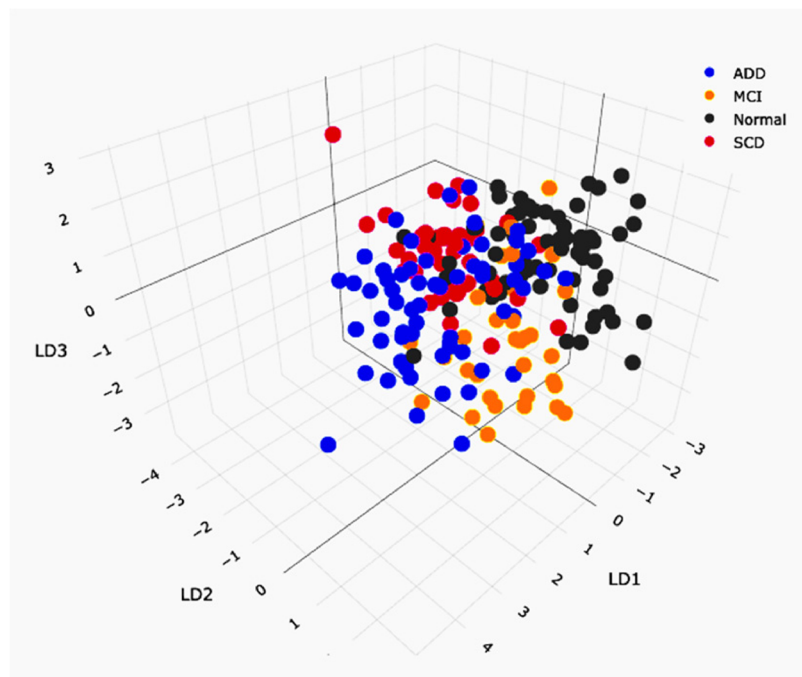


Figure 2. 3D cluster plot created by 3-variable linear discriminant analysis. SCD, subjective cognitive decline; MCI, mild cognitive impairment; ADD, Alzheimer's disease dementia. One can rotate the axis and get the optimal view by using the link <https://rpubs.com/marukocsi/813998>.

hippocampus, education years, plasma $A\beta_{1-42}$ level, and cortical thickness of the right middle cingulate gyrus. We then applied both RF and support vector machine (SVM) classifiers to test

the performance of the 12-feature subset. Finally, we evaluated the performance of models with the area under the receiver operating characteristic curve (AUROC). We first examined

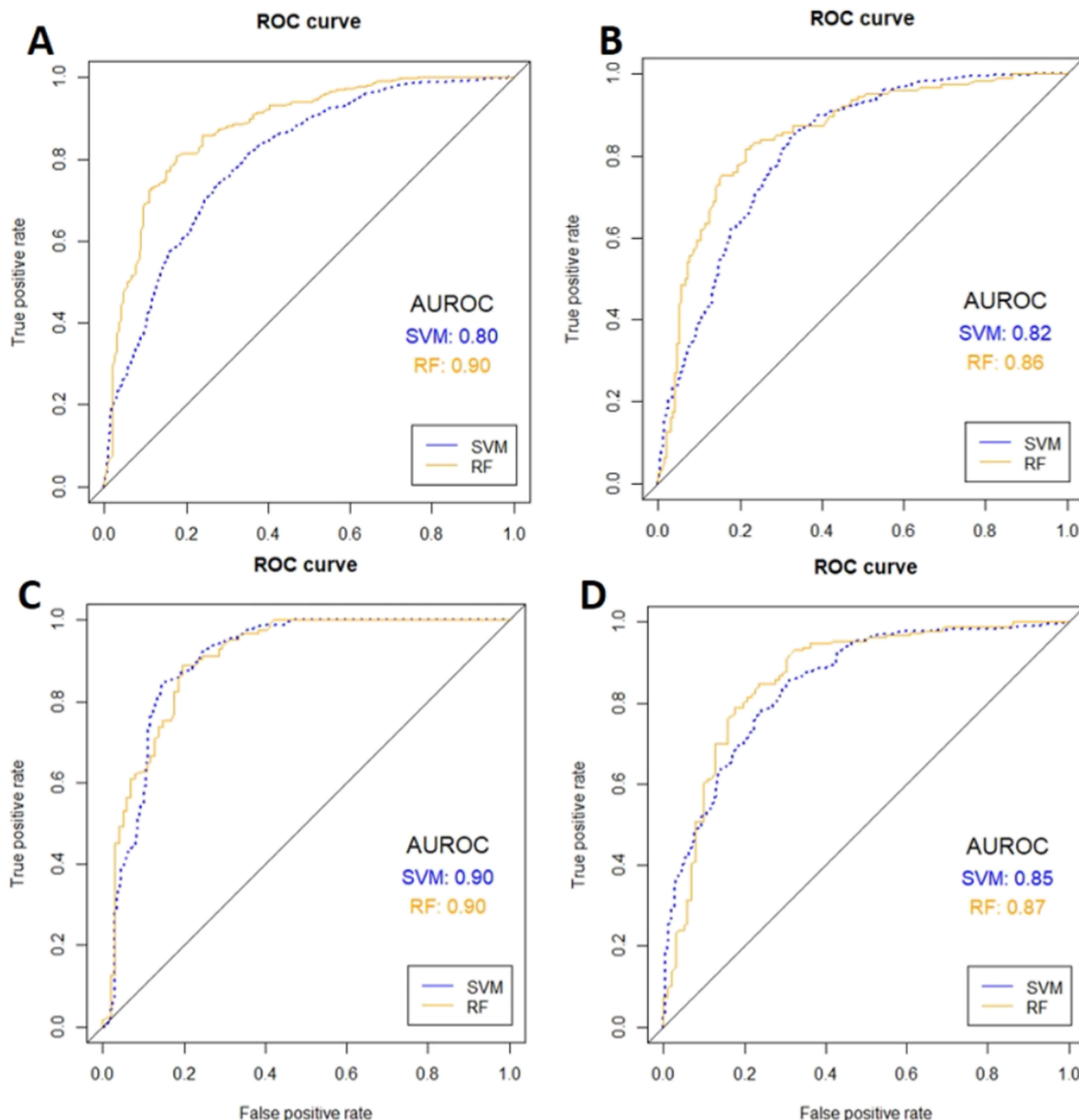


Figure 3. ROC curves using SVM and RF classifiers for a binary taxonomy: (A) between diseases (ADD and MCI) and control; (B) between SCD and control; (C) between MCI and SCD; (D) between MCI and ADD. SCD, subjective cognitive decline; MCI, mild cognitive impairment; ADD, Alzheimer's disease dementia.

the binary taxonomy between the disease group (combining MCI and AD) and the control group. Then we compared each adjacent phase of the AD spectrum, including SCD vs control, MCI vs SCD, and ADD vs MCI.

The binary taxonomy between the disease and control groups, AUROC values were 0.90 [95% confidence interval (CI) 0.86–0.92] for RF and 0.80 (95% CI 0.78–0.82) for SVM (Figure 3A). For the binary taxonomy between SCD and controls, AUROC values were 0.86 (95% CI 0.80–0.92) for RF and 0.82 (95% CI 0.79–0.84) for SVM (Figure 3B). For the binary taxonomy between MCI and SCD, AUROC values were 0.90 (95% CI 0.88–0.92) for RF and 0.90 (95% CI 0.88–0.91) for SVM (Figure 3C). For those between ADD and MCI, AUROC values were 0.87 (95% CI 0.84–0.90) for RF and 0.85 (95% CI 0.84–0.86) for SVM (Figure 3D).

DISCUSSION

With the machine learning algorithms' help, we can differentiate between the clinically defined cognitive unimpaired

controls and diseased subjects (MCI and ADD) with high accuracy (up to AUROCs 0.90). However, from a clinical perspective, it is even more crucial to identify and differentiate subjects in the adjacent clinical phases, such as SCD vs the controls, MCI vs SCD, and ADD vs MCI. The distinction between SCD and the controls was the subjective complaint. The boundary between MCI and SCD was the cognitive performance (including memory) lower than the 4th percentile of their age and education matched control. The point-of-no-return to dementia was the ADL/IADL deterioration in addition to their cognitive deficits. Even experts of dementia frequently encountered difficulty in the differential diagnosis of subjects in the adjacent phases on a clinical ground without the help of comprehensive neuropsychological tests, advanced fluid biomarkers, quantitative structural MR images, or molecular images. The outstanding value of this study is that with the assistance of machine learning algorithms, our selected best 12-feature subset can differentiate between SCD and the controls with the best performance higher than 0.85 AUROCs, between

ADD and MCI higher than 0.85 AUROCs, and between MCI and SCD higher than 0.90 AUROCs. The differentiation between SCD and its adjacent phases, that is, Controls or MCI, is of particular importance since it has been proposed as a pre-MCI at-risk condition of AD. Currently, there are no specific criteria for SCD. In clinical settings, it takes comprehensive, structured interviews relying on personal contact to allow an informed clinical rating of participants' complaints according to diagnostic categories.

Then, let us examine the clinical relevance of the selected best 12-feature subset in a sorted sequence: MMSE score, age, left precuneus cortical thickness, plasma $\text{A}\beta_{1-40}$ level, left hippocampus volume, right angular gyrus cortical thickness, entorhinal gyrus cortical thickness, plasma total tau levels, right hippocampus volume, education years, plasma $\text{A}\beta_{1-42}$ levels, and cortical thickness of the right middle cingulate gyrus. MMSE is a concise and clinically useful tool for measuring global cognitive function. However, it has ceiling and floor effects even after adjustment for the educational level.³⁷ In AD studies, it is commonly encountered that participants in the ADD group were significantly older than those in control and MCI groups as in this study. Age is always a risk factor for both MCI and dementia.³⁸ As for the plasma biomarkers, our previous research has shown that plasma $\text{A}\beta_{40}$ might be a protective indicator of less brain amyloid deposition and cortical atrophy,³⁹ and computed products of $\text{A}\beta_{1-42}$ and tau may be a predictor of AD.^{28,40} Plasma total tau was negatively correlated with hippocampus brain volume and precuneus cortical thickness in MCI and AD.^{41,42} On the other hand, previous research showed brain structural change even in subjects with SCD,⁴³ especially those clinical-based samples as in this study.^{43,44}

We used LOOCV to estimate the performance of our model construction procedure, which is particularly important since our data set is not too big for LOOCV, which is an unbiased version of cross-validation. LOOCV is an estimate of a model's generalization performance trained on $n - 1$ samples of data, which is one sample estimate of a model's performance trained on all n samples.

The strength of the present report is twofold. First, the machine learning system can differentiate clinical gray zones using easily accessible plasma biomarkers and clinically available brain MR structural images. As aforementioned, it is not always easy, even in an expert's service, to define taxonomies such as control vs SCD, SCD vs MCI, and MCI vs mild ADD without a comprehensive neuropsychological test, functional assessment from careful observation of a responsible principal caregiver, relative invasive CSF biomarkers, or expensive PET scans with radiation risk. The other strength is that we can achieve such good accuracy (Table S1) even with a relatively small number of subjects in each subgroup. Moreover, with the combination of those selected features (variables) by machine learning algorithms, we achieved high AUROC (0.85~0.92) corresponding to a considerable effect size (1.44~2.01),⁴⁵ implying a very significant synergistic diagnostic effect between features.

There is an unexpected finding. Intuitively, clinical differentiation between MCI and SCD is more complex than distinguishing control from disease (MCI/ADD). However, our results show that the AUROCs are about equal (RF 0.90 for both MCI vs SCD and disease vs control) or the AUROCs of MCI vs SCD are greater than disease vs control (SVM 0.90 vs 0.80). The exact cause is unclear. We proposed that, at least

in part, is due to sampling bias. The SCD group (14.5 ± 4.1 years) has a higher education than the MCI group (11.5 ± 4.7 years, $p < 0.01$). In addition, SCD is a more homogenous group than other groups in terms of standard deviations of MMSE scores, total tau, and $\text{A}\beta_{1-40}$ levels (Table 1). MMSE (top 1), $\text{A}\beta_{1-40}$ (top 4), total tau (top 8), and education (top 10) are among the top 10 features, which might contribute to the distinction between SCD and MCI.

Limitation of the Study. Our study has several limitations. First, due to the scarcity of human data, our study population is still relatively small to avoid all possible sampling bias, and we cannot have an additional validation cohort at this moment. Therefore, we must take great care in generalizing our study's findings. Also, this is a cross-sectional study, and validation through observation of natural course is not available. Therefore, in the future, we need to repeat the study using biomarkers and machine learning algorithms of this report on a novel population for cross-validation and a longitudinal cohort composing cognitively unimpaired and AD subjects with different clinical severities.

Conclusions. We can differentiate the gray zone between adjacent AD phases with easily accessible plasma biomarkers and clinically available brain MR structural images and achieve a significant effect size with machine learning algorithms. Future application on participant inclusion of appropriate subjects with preclinical, prodromal, or early AD for preventive intervention or disease-modifying therapy will be possible.

METHODS AND MATERIAL

Subjects. In total, we recruited 206 subjects from the memory clinic of the Department of Neurology, National Taiwan University Hospital. They included 69 cognitively unimpaired control subjects, 40 SCD, 34 MCI (mostly multi-domain), and 63 ADD (Table 1). This study adhered to the National Institute on Aging/Alzheimer's Association Diagnostic Guidelines for MCI and dementia due to AD.^{21,22} The subjects were required to have had at least 6 years of formal education or read and write Chinese to complete the comprehensive neuropsychological battery (NPT). Subjects with cognitive decline complaints but unimpaired cognitive performance (better than -1.5 SD of their age- and education-matched norm) were categorized as the SCD group.⁵ The MCI group had abnormal performance in the NPT, defined as lower than the 4th percentile compared with their age- and education-matched controls for more than one memory task²³ with or without impairment in other cognitive domains. In addition, they had normal instrumental ADL. Subjects with impaired cognitive function and abnormal instrumental ADL were classified as ADD.²⁴ We excluded those subjects whose brain MR images showed main artery strokes or microangiopathy (Fazekas score >1 or lacunar infarcts) for possible confounding of vascular cognitive impairment.

Neuroimage Biomarkers. Image Acquisition. High-resolution structural brain magnetic resonance imaging (MRI) data were acquired using a 1.5 T MRI scanner (EXCITE, General Electric, Milwaukee, WI, USA). A whole-brain T1-weighted 3D spoiled gradient recovery sequence was used (TE = 9.4 ms, TR = 3.9 ms, T1 = 600 ms, flip angle = 12 degrees, matrix size = 192 X 192, FOV = 25 cm), and a total of 170 contiguous sagittal slices, 1.3 mm in height, were acquired.

We also acquired routine clinical MR images from the same scanner with axial T2 (TR = 1067 ms, TE = 35 ms, flip angle = 20°) and axial T2 FLAIR (TR = 8600 ms, TE = 114.3 ms, flip angle = 90°) for diagnostic purposes.

Image Processing. T1 images were processed using FreeSurfer suite, version 5.2 (<https://surfer.nmr.mgh.harvard.edu>). The image processing steps included motion correction and conformation, Talairach transform computation, intensity normalization, volumetric

registration, and white matter segmentation, followed by spherical mapping and registration, then cortical parcellation, and mapping to subcortical segmentation.²⁵ Afterward, we selected and extracted the cortical thickness data from 16 cortical areas, including anterior, middle, and posterior cingulate cortices, precuneus, angular gyrus, entorhinal, perirhinal, parahippocampus cortices of the bilateral hemispheres, and the volumes of bilateral hippocampi for analysis.²⁶

Plasma Biomarkers. *Preparation of Human Plasma.* Subjects were asked to provide a 10-mL non-fasting venous blood sample (K3 EDTA, lavender top tube). The blood samples were centrifuged (2500 g for 15 min) within 1 h of collection, and the plasma was aliquoted into cryotubes and stored at -80 °C.

Assays of Plasma Biomarkers. All human plasma samples were measured for A β ₁₋₄₂, A β ₁₋₄₀, and tau protein using immunomagnetic reduction assay (IMR) with three different reagents. Each reagent consists of magnetic nanoparticles dispersed in a pH 7.2 phosphoryl buffer solution. These reagent nanoparticles are produced by immobilizing antibodies against A β ₁₋₄₀ (Sigma/A3981), A β ₁₋₄₂ (Abcam/ab34376), and tau protein (Sigma/T9450) on magnetic nanoparticles produced by MagQu Co. Ltd., New Taipei City, Taiwan. The mean diameter of antibody-functionalized magnetic nanoparticles is 50–60 nm. The magnetic concentration of each kind of reagent is 12 mg-Fe/mL. For a given human plasma sample, we mixed 80 μ L of A β ₁₋₄₀ reagent (MFAB0-0060, MagQu) with 40 mL of room-temperature human plasma; 60 μ L of A β ₁₋₄₂ reagent (MF-AB2-0060, MagQu) with 60 μ L plasma; and 80 μ L of total tau reagent (MF-TAU-0060, MagQu) with 40 μ L plasma. The reduction in the ac magnetic susceptibility, that is, the IMR signal of the reagent after being mixed with a sample, was measured using a superconducting quantum interference device-based ac magnetic susceptometer (XacPro-S, MagQu). We converted IMR signals to concentrations of biomarkers by using logistic functions. Duplicate measurements of IMR signals were performed for each human plasma sample. The mean value of the duplicated measurements for a given biomarker in a human plasma sample was used for the statistical analysis. The IMR assay of plasma biomarkers for the AD spectrum was detailed in our previous work.^{27–29}

Data Set Description. In total, there are 26 features (inputs) of the data set, including 3 demographic characteristics (age, gender, and education), 2 clinical statuses (MMSE and CDR scores), 18 AD-signature image-biomarker areas (detailed in the paragraph above),²³ and 3 plasma AD biomarkers (A β ₁₋₄₀, A β ₁₋₄₂, and total tau concentrations measured by IMR). Although the AB42/AB40 ratio can be a good indicator, we have used this ratio in our previous study to differentiate between MCI and ADD.²⁹ However, the AB42/AB40 ratio, on the one hand, is a derived value; on the other hand, it has a high positive correlation with A β ₁₋₄₂ ($r = 0.88$) and a high negative correlation with A β ₁₋₄₀ ($r = -0.66$). Hence, the ratio is not included as an input variable. Furthermore, we used CDR total or memory sub-box scores for clinical classifications. Thus, it is close to the "ground truth", and we removed the CDR feature in our proposed model.³⁰ On the other hand, although MMSE is a global cognitive function assessment, it is culture- and education-dependent; its score provides a reference for clinical classification. Thus, we included 25 features in total for the training of algorithms.

We used multivariate imputation by chained equations (MICE)³¹ and classification and regression trees (CART)³² to handle missing values. MICE created multiple imputations (replacement values) for multivariate missing data. Each incomplete column must be a target column with its specific set of predictors. We used the CART algorithm as the predictor and imputed 58 values by MICE. The percentage of imputation is 0.01%. We operated data adjustment to make the data set more compliant with machine learning, and we used standard scores (z-scores) to adjust the features.

Dimensionality Reduction. In machine learning, dimensionality reduction reduces the number of features such that it retains the characteristics of the reduced data as much as possible. Principal component analysis (PCA) and LDA are two popular dimensionality reduction methods used on data with many input features. However, PCA is a commonly used unsupervised linear transformation

technique, and LDA is a supervised method that considers class labels when reducing the number of dimensions. Our data set contains class labels and subjects assigned as SCD, MCI, or ADD; thus, LDA is a more appropriate method for our data set.

This report used both feature selection and feature extraction for dimensionality reduction. Both methods can avoid the curse of dimensionality.

Feature Extraction. Feature extraction is a process of dimensionality reduction by which an initial data set is reduced to more manageable groups for processing. Feature extraction aims to reduce the number of features in a data set by creating new features from the existing ones. We used the LDA method as the feature extraction technique. As mentioned above, LDA is among the most commonly used dimensionality reduction techniques in the preprocessing step for pattern classification and machine learning applications. LDA projects a data set onto a lower-dimensional space with good class separability to avoid overfitting and reduce computational costs. However, classical LDA performs poorly in high-dimension data corresponding to the sample covariance matrix's singularity and instability. Therefore, we would employ LDA for the initial reduction of data dimensionality and visualization of the data set in a 3D scatter plot in this study.

Feature Selection. Feature selection selects the best features among all features that are useful to discriminate classes.¹⁹ In feature selection, we used a SFS wrapper method to enhance dimensionality reduction.¹⁹ The SFS method is an efficient feature selection algorithm to classify biological signals.³³ The SFS is an iterative method, in which we start with having no feature in the model. For the first step, the best single feature is selected. Then, pairs of features are formed using one of the remaining features, and it is the best feature of the remaining features, and the best pair is selected. Next, triplets of features are formed using one of the remaining features and these two best features, and the best triplet is selected. This procedure continues until it establishes a predefined number of features. Therefore, we kept adding the feature that best improved our model (Figure 4).

Classification Algorithms. Among benchmark deep-learning classifiers,³⁴ our previous study¹⁵ shows that overall speaking, RF³⁵ and SVM³⁶ produce the best accuracy. Therefore, we used R language to implement RF and SVM classifiers.

Statistical Analysis. Between-group comparison of nonparametric data such as gender distribution was examined by the chi-square test. In addition, the between-group comparison of parametric data

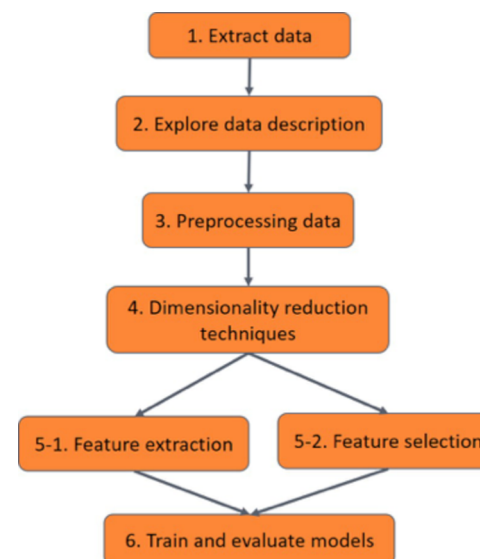


Figure 4. Flow chart, including data preprocessing, dimensionality reduction, feature extraction, feature selection, and training machine learning classification models of this study.

was analyzed by multivariate analysis of covariance, controlling the age effect with Bonferroni correction of multiple comparisons.

ASSOCIATED CONTENT

Supporting Information

The Supporting Information is available free of charge at <https://pubs.acs.org/doi/10.1021/acschemneuro.2c00255>.

Accuracy of LDA1, LDA1 + 2, LDA1 + 2 + 3 by support vector machine and random forest and performance of different classifiers on the binary taxonomy ([PDF](#))

AUTHOR INFORMATION

Corresponding Author

Ming-Jang Chiu — Department of Neurology, College of Medicine, National Taiwan University Hospital, National Taiwan University, Taipei 100225, Taiwan; Graduate Institute of Biomedical Electronics and Bioinformatics and Graduate Institute of Psychology, National Taiwan University, Taipei 106319, Taiwan; Graduate Institute of Brain and Mind Sciences, National Taiwan University, Taipei 100233, Taiwan; orcid.org/0000-0002-4158-4423; Phone: +886-2-23123456 ext. 265339; Email: mjchiu@ntu.edu.tw

Authors

Shu-I Chiu — Department of Computer Science, National Chengchi University, Taipei 116302, Taiwan
Ling-Yun Fan — Queensland Brain Institute, University of Queensland, St Lucia, QLD 4067, Australia; Departments of Neurology, National Taiwan University Hospital Bei-Hu Branch, Taipei 108206, Taiwan
Chin-Hsien Lin — Department of Neurology, College of Medicine, National Taiwan University Hospital, National Taiwan University, Taipei 100225, Taiwan
Ta-Fu Chen — Department of Neurology, College of Medicine, National Taiwan University Hospital, National Taiwan University, Taipei 100225, Taiwan
Wee Shin Lim — Department of Computer Science and Information Engineering, National Taiwan University, Taipei 106319, Taiwan
Jyh-Shing Roger Jang — Department of Computer Science and Information Engineering, National Taiwan University, Taipei 106319, Taiwan

Complete contact information is available at:
<https://pubs.acs.org/10.1021/acschemneuro.2c00255>

Author Contributions

Conceptualization, M.-J.C.; methodology, M.-J.C. and S.-I.C.; software, S.-I.C. and J.-S.R.J.; analysis, M.-J.C. and S.-I.C.; data curation, S.-I.C., L.-Y.F., T.-F.C., and M.-J.C.; writing—original draft preparation, M.-J.C. and S.-I.C.; writing—review and editing, J.-S.R.J. and M.-J.C.; visualization, M.-J.C. and S.-I.C.; supervision, M.-J.C.; project administration, M.-J.C.; funding acquisition, M.-J.C.

Funding

The research was supported by National Science and Technology Council (111-2314-B-002-282); and the article processing charge was supported by Yuanta foundation (2021–2023).

Notes

The authors declare no competing financial interest.

This study was approved by the National Taiwan University Hospital's institutional ethics board committee (201406125DSC, 20160470 MINC, and NTUH 201903094RINA). All participants or their proxies provided informed consent to participate in the study.

All authors have read and approved the manuscript in this final form.

ACKNOWLEDGMENTS

We are grateful to all the participants in this study.

REFERENCES

- (1) Morris, J. C. Early-stage and preclinical Alzheimer's disease. *Alzheimer Dis. Assoc. Disord.* **2005**, *19*, 163–165.
- (2) Roberts, R.; Knopman, D. S. Classification and epidemiology of MCI. *Clin. Geriatr. Med.* **2013**, *29*, 753–772.
- (3) McGuinness, B.; Barrett, S. L.; McIlvenna, J.; Passmore, A. P.; Shorter, G. W. Predicting conversion to dementia in a memory clinic: A standard clinical approach compared with an empirically defined clustering method (latent profile analysis) for mild cognitive impairment subtyping. *Alzheimers Dement. (Amst)* **2015**, *1*, 447–454.
- (4) Jessen, F.; Amariglio, R. E.; van Boxtel, M.; Breteler, M.; Ceccaldi, M.; Chetelat, G.; et al. A conceptual framework for research on subjective cognitive decline in preclinical Alzheimer's disease. *Alzheimer's Dement.* **2014**, *10*, 844–852.
- (5) Molinuevo, J. L.; Rabin, L. A.; Amariglio, R.; Buckley, R.; Dubois, B.; Ellis, K. A.; et al. Implementation of subjective cognitive decline criteria in research studies. *Alzheimer's Dement.* **2017**, *13*, 296–311.
- (6) Abner, E. L.; Kryscio, R. J.; Caban-Holt, A. M.; Schmitt, F. A. Baseline subjective memory complaints associated with increased risk of incident dementia: the PRE ADVICE trial. *J. Prev. Alzheimers Dis.* **2015**, *2*, 11–16.
- (7) Donovan, N. J.; Amariglio, R. E.; Zoller, A. S.; Rudel, R. K.; Gomez-Isla, T.; Blacker, D.; et al. Subjective cognitive concerns and neuropsychiatric predictors of progression to the early clinical stages of Alzheimer disease. *Am. J. Geriatr. Psychiatry* **2014**, *22*, 1642–1651.
- (8) Reisberg, B.; Shulman, M. B.; Torossian, C.; Leng, L.; Zhu, W. Outcome over seven years of healthy adults with and without subjective cognitive impairment. *Alzheimer's Dement.* **2010**, *6*, 11–24.
- (9) Jessen, F.; Wolfgruber, S.; Wiese, B.; Bickel, H.; Mosch, E.; Kaduszkiewicz, H.; et al. AD dementia risk in late MCI, in early MCI, and in subjective memory impairment. *Alzheimer's Dement.* **2014**, *10*, 76–83.
- (10) Sperling, R. A.; Aisen, P. S.; Beckett, L. A.; Bennett, D. A.; Craft, S.; Fagan, A. M.; et al. Toward defining the preclinical stages of Alzheimer's disease: recommendations from the National Institute on Aging-Alzheimer's Association workgroups on diagnostic guidelines for Alzheimer's disease. *Alzheimer's Dement.* **2011**, *7*, 280–292.
- (11) Katako, A.; Shelton, P.; Goertzen, A. L.; Levin, D.; Bybel, B.; Aljuaid, M.; et al. Machine learning identified an Alzheimer's disease-related FDG-PET pattern which is also expressed in Lewy body dementia and Parkinson's disease dementia. *Sci. Rep.* **2018**, *8*, 13236.
- (12) Kloppel, S.; Stonnington, C. M.; Chu, C.; Draganski, B.; Scahill, R. I.; Rohrer, J. D.; et al. Automatic classification of MR scans in Alzheimer's disease. *Brain* **2008**, *131*, 681–689.
- (13) Lee, S. H.; Bachman, A. H.; Yu, D.; Lim, J.; Ardekani, B. A.; Alzheimer's Disease Neuroimaging Initiative. Predicting progression from mild cognitive impairment to Alzheimer's disease using longitudinal callosal atrophy. *Alzheimers Dement. (Amst)* **2016**, *2*, 68–74.
- (14) Davatzikos, C.; Resnick, S. M.; Wu, X.; Parmpi, P.; Clark, C. M. Individual patient diagnosis of AD and FTD via high-dimensional pattern classification of MRI. *Neuroimage* **2008**, *41*, 1220–1227.
- (15) Lin, C. H.; Chiu, S. I.; Chen, T. F.; Jang, J. R.; Chiu, M. J. Classifications of Neurodegenerative Disorders Using a Multiplex Blood Biomarkers-Based Machine Learning Model. *Int. J. Mol. Sci.* **2020**, *21*, 6914.

- (16) Khalid, S.; Khalil, T.; Nasreen, S. editors. A survey of feature selection and feature extraction techniques in machine learning. *2014 Science and Information Conference*; IEEE, 2014.
- (17) Janecek, A.; Gansterer, W.; Demel, M.; Ecker, G., editors. *On the relationship between feature selection and classification accuracy. New challenges for feature selection in data mining and knowledge discovery*; 2008.
- (18) Chiu, S.-I.; Lin, C.-H.; Lim, W. S.; Chiu, M.-J.; Chen, T.-F.; Jang, J.-S. R. editors. Predicting Neurodegenerative Diseases Using a Novel Blood Biomarkers-based Model by Machine Learning. In *2019 International Conference on Technologies and Applications of Artificial Intelligence (TAII)*; IEEE, 2019.
- (19) Remeseiro, B.; Bolon-Canedo, V. A review of feature selection methods in medical applications. *Comput. Biol. Med.* **2019**, *112*, No. 103375.
- (20) Whitney, A. W. A direct method of nonparametric measurement selection. *IEEE Trans. Comp.* **1971**, *C-20*, 1100–1103.
- (21) McKhann, G. M.; Knopman, D. S.; Chertkow, H.; Hyman, B. T.; Jack, C. R., Jr.; Kawas, C. H.; et al. The diagnosis of dementia due to Alzheimer's disease: recommendations from the National Institute on Aging-Alzheimer's Association workgroups on diagnostic guidelines for Alzheimer's disease. *Alzheimer's Dement.* **2011**, *7*, 263–269.
- (22) Albert, M. S.; DeKosky, S. T.; Dickson, D.; Dubois, B.; Feldman, H. H.; Fox, N. C.; et al. The diagnosis of mild cognitive impairment due to Alzheimer's disease: recommendations from the National Institute on Aging-Alzheimer's Association workgroups on diagnostic guidelines for Alzheimer's disease. *Alzheimer's Dement.* **2011**, *7*, 270–279.
- (23) Lezak, M. D.; Howieson, D. B.; Loring, D. W. *Neuropsychological assessment* (4th ed.); Oxford University Press: New York, (2004).
- (24) Mao, H. F.; Chang, L. H.; Tsai, A. Y.; Huang, W. W.; Tang, L. Y.; Lee, H. J.; Sun, Y.; Chen, T. F.; Lin, K. N.; Wang, P. N.; Shyu, Y. I. L.; Chiu, M. J. Diagnostic accuracy of Instrumental Activities of Daily Living for dementia in community-dwelling older adults. *Age Ageing* **2018**, *47*, 551–557.
- (25) (a) Fischl, B.; Salat, D. H.; Busa, E.; Albert, M.; Dieterich, M.; Haselgrave, C.; van der Kouwe, A.; Killiany, R.; Kennedy, D.; Klaveness, S.; Montillo, A.; Makris, N.; Rosen, B.; Dale, A. M. Whole brain segmentation: automated labeling of neuroanatomical structures in the human brain. *Neuron* **2002**, *33*, 341–355. (b) Fischl, B. FreeSurfer. *Neuroimage* **2012**, *62*, 774–781.
- (26) Dickerson, B. C.; Stoub, T. R.; Shah, R. C.; Sperling, R. A.; Killiany, R. J.; Albert, M. S.; et al. Alzheimer-signature MRI biomarker predicts AD dementia in cognitively normal adults. *Neurology* **2011**, *76*, 1395–1402.
- (27) Chiu, M. J.; Yang, S. Y.; Chen, T. F.; Chieh, J. J.; Huang, T. Z.; Yip, P. K.; et al. New assay for old markers-plasma beta-amyloid of mild cognitive impairment and Alzheimer's disease. *Curr. Alzheimer Res.* **2012**, *9*, 1142–1148.
- (28) Chiu, M. J.; Yang, S. Y.; Horng, H. E.; Yang, C. C.; Chen, T. F.; Chieh, J. J.; et al. Combined plasma biomarkers for diagnosing mild cognition impairment and Alzheimer's disease. *ACS Chem. Neurosci.* **2013**, *4*, 1530–1536.
- (29) Chiu, M. J.; Chen, T. F.; Hu, C. J.; Yan, S. H.; Sun, Y.; Liu, B. H.; Chang, Y. T.; Yang, C. C.; Yang, S. Y. Nanoparticle-based immunomagnetic assay of plasma biomarkers for differentiating dementia and prodromal stages of Alzheimer's disease - A cross-validation study. *Nanomedicine* **2020**, *28*, No. 102182.
- (30) Carlotto, M. J. Effect of errors in ground truth on classification accuracy. *Int. J. Remote Sens.* **2009**, *30*, 4831–4849.
- (31) Buuren, S. V.; Groothuis-Oudshoorn, K. mice: Multivariate imputation by chained equations in *R. J. Stat. Softw.* **2011**, *45*, 1–68.
- (32) Breiman, L.; Friedman, J.; Stone, C. J.; Olshen, R. A. *Classification and regression trees*; CRC press, 1984.
- (33) Phinyomark, A. N.; Khushaba, R.; Scheme, E. Feature extraction and selection for myoelectric control based on wearable EMG sensors. *Sensors* **2018**, *18*, 1615.
- (34) Wu, X.; Kumar, V.; Quinlan, J. R.; Ghosh, J.; Yang, Q.; Motoda, H.; et al. Top 10 algorithms in data mining. *Knowl. Inf. Syst.* **2008**, *14*, 1–37.
- (35) Ho, T. K., editor *Random decision forests. Proceedings of 3rd international conference on document analysis and recognition*; IEEE, 1995.
- (36) (a) Cortes, C.; Vapnik, V. Support-vector networks. *Mach. Learn.* **1995**, *20*, 273–297. (b) Abe, S. *Support vector machines for pattern classification*; Springer; 2005.
- (37) Franco-Marina, F.; Garcia-Gonzalez, J. J.; Wagner-Echeagaray, F.; Gallo, J.; Ugalde, O.; Sanchez-Garcia, S.; et al. The Mini-mental State Examination revisited: ceiling and floor effects after score adjustment for educational level in an aging Mexican population. *Int. Psychogeriatr.* **2010**, *22*, 72–81.
- (38) Sun, Y.; Lee, H. J.; Yang, S. C.; Chen, T. F.; Lin, K. N.; Lin, C. C.; et al. A nationwide survey of mild cognitive impairment and dementia, including very mild dementia, in Taiwan. *PLoS One* **2014**, *9*, No. e100303.
- (39) Fan, L. Y.; Tzen, K. Y.; Chen, Y. F.; Chen, T. F.; Lai, Y. M.; Yen, R. F.; et al. The Relation Between Brain Amyloid Deposition, Cortical Atrophy, and Plasma Biomarkers in Amnesic Mild Cognitive Impairment and Alzheimer's Disease. *Front. Aging Neurosci.* **2018**, *10*, 175.
- (40) Lue, L. F.; Sabbagh, M. N.; Chiu, M. J.; Jing, N.; Snyder, N. L.; Schmitz, C.; Guerra, A.; Belden, C. M.; Chen, T. F.; Yang, C. C.; Yang, S. Y.; Walker, D. G.; Chen, K.; Reiman, E. M. Plasma Levels of Abeta42 and Tau Identified Probable Alzheimer's Dementia: Findings in Two Cohorts. *Front. Aging Neurosci.* **2017**, *9*, 226.
- (41) Deters, K. D.; Risacher, S. L.; Kim, S.; Nho, K.; West, J. D.; Blennow, K.; et al. Plasma Tau Association with Brain Atrophy in Mild Cognitive Impairment and Alzheimer's Disease. *J. Alzheimers Dis.* **2017**, *58*, 1245–1254.
- (42) Chiu, M. J.; Chen, Y. F.; Chen, T. F.; Yang, S. Y.; Yang, F. P.; Tseng, T. W.; Chieh, J. J.; Chen, J. C. R.; Tzen, K. Y.; Hua, M. S.; Horng, H. E. Plasma tau as a window to the brain-negative associations with brain volume and memory function in mild cognitive impairment and early Alzheimer's disease. *Hum. Brain Mapp.* **2014**, *35*, 3132–3142.
- (43) Fan, L. Y.; Lai, Y. M.; Chen, T. F.; Hsu, Y. C.; Chen, P. Y.; Huang, K. Z.; et al. Diminution of context association memory structure in subjects with subjective cognitive decline. *Hum. Brain Mapp.* **2018**, *39*, 2549–2562.
- (44) Pini, L.; Wennberg, A. M. Structural imaging outcomes in subjective cognitive decline: Community vs. clinical-based samples. *Exp. Gerontol.* **2021**, *145*, No. 111216.
- (45) Rice, M. E.; Harris, G. T. Comparing effect sizes in follow-up studies: ROC Area, Cohen's d, and r. *Law Hum. Behav.* **2005**, *29*, 615–620.